APPENDIX B

A PLATE WITH AN INTERNAL FLAW UNDER EXTENSION OR BENDING

1. Introduction

Some of the common flaws in pipe welds are planar internal flaws. In studying the question of flaw evaluation in pipes containing multiple flaws, an important problem is therefore the problem of interaction between the internal planar flaws and between flaws and the free surfaces. The general three-dimensional elasticity problem is, at the present time, analytically intractable. However, the previous studies show that the application of the "line spring" model to surface cracks in plates and shells seems to give results which agree with very limited existing finite element results reasonably well [1,2].

The objective of this study is to extend the application of the line spring model to internal cracks and, by comparing the results with the existing finite element solutions, to establish its degree of accuracy. The broader aim is, of course, to use the technique in the interaction problems of multiple internal cracks the solution of which is needed and is not available. After solving the single crack problem and showing that the stress intensity factors compare quite well with the existing solutions, extensive results are obtained for an internal crack with an elliptic or a rectangular boundary in a plate under extension or bending.

2. ~~On the~~ Formulation of the Problem

The formulation of the general problem follows very closely the treatment given in [1]. In the special symmetric crack geometry and symmetric loading shown in Fig. 1 the tension and bending problems are uncoupled. Thus, the integral equations given in [1] would also be uncoupled and the formulation and the method of solution would remain

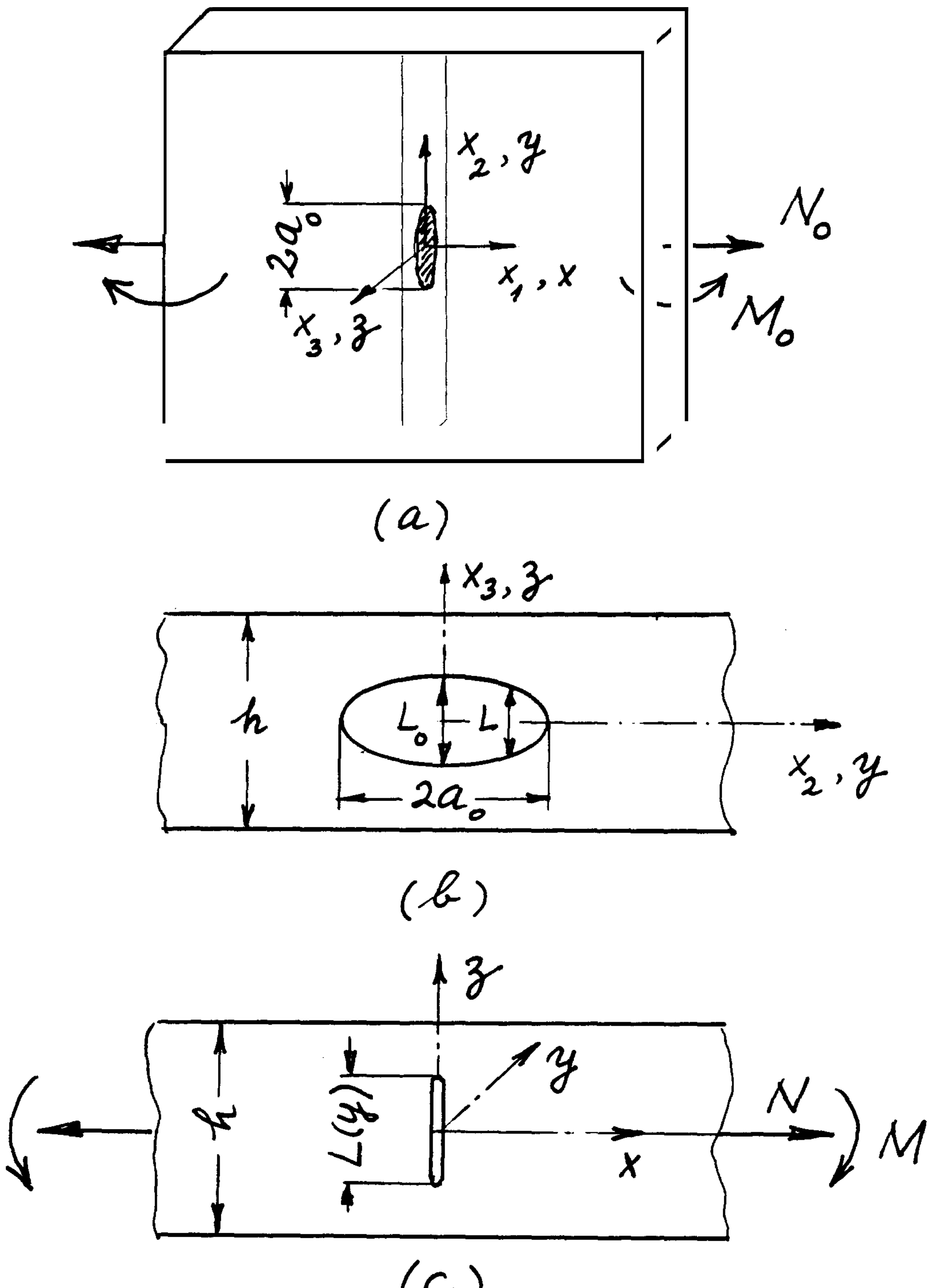

Fig. 1 Geometry and notation for a plate containing an internal planar crack.

the same. However, in order to solve the problem new stress intensity shape functions g_t and g_b for the new crack geometry under consideration are needed. In terms of these functions the Mode I stress intensity factor K along the crack front is given by

$$K(y) = \sqrt{h}\,[g_t\sigma(y) + g_b m(y)] \qquad (1)$$

where g_t and g_b are functions of L/h and σ and m are defined by

$$\sigma(y) = \frac{N(y)}{h}\ , \quad m(y) = \frac{6M(y)}{h^2}\ . \qquad (2)$$

In (1) and (2) y is the coordinate along the crack normalized with respect to the half crack length a_o, i.e., $y = x_2/a_o$ (Fig. 1 a,b), and N(y) and M(y) are membrane and bending resultants along the net ligament (Fig. 1c).

The unknown functions $\sigma(y)$ and m(y) are determined after solving the integral equations [1], whereas the shape functions g_t and g_b are obtained from the corresponding plane strain problem (Fig. 1c). The stress intensity factors K_N and K_M obtained from the solution of the plane strain problem described in Fig. 1c under membrane and bending resultants N and M are given by Table 1 [3].

Table 1. Stress intensity factors for centrally cracked plate subjected to tension (N) or bending (M) under plane strain conditions. ($\sigma=N/h$, $m=6M/h^2$)

L/h	$\frac{K_N}{\sigma\sqrt{\pi L/2}}$	$\frac{K_M}{m\sqrt{\pi L/2}}$
0.05		0.1500
0.1	1.0060	0.3000
0.2	1.0246	0.6004
0.3	1.0577	0.9031
0.4	1.1094	1.2135
0.5	1.1867	1.5435
0.6	1.3033	1.9179
0.7	1.4884	2.3918
0.8	1.8169	3.1113
0.9	2.585	4.6653
0.95	4.252	6.8526

In order to use in the analysis the results given in Table 1 must be represented by analytic expressions. Thus, from (1) observing that

$$K = K_N + K_M ,$$

$$K_N = \sigma\sqrt{h}\ g_t , \quad K_M = m\sqrt{h}\ g_b \tag{3}$$

and by expressing

$$g_t(L/h) = \sqrt{\pi L/h} \sum_{j=1}^{n} b_j (L/h)^{2(j-1)} , \tag{4}$$

$$g_b(L/h) = \sqrt{\pi L/h} \sum_{j=1}^{n} c_j (L/h)^{j-1} . \tag{5}$$

The coefficients b_j and c_j may be obtained by curve-fitting (see Table 2).

3. The Results ~~for a~~ Single Crack

In the analysis used for the present study the contour of the planar crack described by $L = L(x_2)$ or $L = L(y)$ can be any function. If,

Table 2. The coefficients b_j and c_j for the shape functions g_t and g_b (Eqs. 4 and 5).

j	b_j	c_j
1	0.7071	0.1013
2	0.4325	-2.7775
3	-0.1091	90.3734
4	7.3711	-862.4307
5	-57.7894	4843.4692
6	271.1551	-17069.1142
7	-744.4204	38813.4897
8	1183.9529	-56865.3055
9	-1001.4920	51832.6941
10	347.9786	-26731.2995
11		5959.4888

however, some subcritical crack growth takes place in the medium, the. contour defining the crack is usually a convex smooth function. Here we will give examples for two contours, namely an ellipse and a rectangle, which roughly speaking may be considered as the two limiting cases for the shape such an internal crack may assume. The ellipse is defined by

$$(x_2/a_0)^2 + x_3^2/(L_0/2)^2 = 1 \tag{6}$$

or

$$x_2 = a_0 \cos\theta \quad , \quad x_3 = (L_0/2) \sin\theta \tag{7}$$

which, by observing that $x_2/a_0 = y$ and $L(y) = 2x_3$ (Fig. 1b), gives the function $L(y)$ as follows

$$L(y) = L_0\sqrt{1-y^2} \quad , \quad (-1<y<1). \tag{8}$$

For a rectangular contour it is simply assumed that $L(y) = L_0$, $(-1<y<1)$. The stress intensity factors for a single crack calculated from (3) after solving the integral equations and determining the functions $\sigma(y)$ and $m(y)$ are given in Tables 3-7 and Figures 2-9.

Table 3 shows the comparison between the stress intensity factor at the midsection of a long internal elliptic crack (i.e., for $y=0$, $L=L_0$, $a_0<\infty$) and that obtained from the corresponding plane strain solution (i.e., Table 1 or equations (3) and (4) with $\sigma=\sigma_0$, $L=L_0$, $a_0=\infty$) in a plate under uniform tension σ_0 perpendicular to the crack surface(*). Note that, as expected, the stress intensity factors $K(L_0)$ for the

---

*) K_∞ shown in Table 3 is calculated from Eqs. (3) and (4) by using the coefficients b_j given in Table 2. Comparison of K_∞ of Table 3 and K_N of Table 1 gives some idea about the accuracy of the curve fitting, Eq. (4).

Table 3. Comparison of the stress intensity factor. $K(L_0)$ at the center of an internal elliptic crack of length $2a_0$ with the corresponding plane strain value K_∞ (for which $a_0=\infty$) in a plate under uniform membrane stress $\sigma_0=N_0/h$.

L_0/h	$\frac{K_\infty}{\sigma_0\sqrt{\pi L_0/2}}$ $(a_0/L_0=\infty)$	$\frac{K(L_0)}{\sigma_0\sqrt{\pi L_0/2}}$			$100\,\frac{K(L_0)-K_\infty}{K_\infty}$		
		$a_0/L_0=10$	$a_0/L_0=20$	$a_0/L_0=100$	$a_0/L_0=10$	$a_0/L_0=20$	$a_0/L_0=100$
0.1	1.005997	0.999043	0.995528	0.997353	-0.7	-1.0	-0.9
0.2	1.024588	1.013152	1.011516	1.015310	-1.1	-1.3	-0.9
0.3	1.057743	1.041450	1.041460	1.047558	-7.5	-1.5	-1.0
0.4	1.109368	1.091117	1.089049	1.098079	-1.6	-1.8	-1.0
0.5	1.186659	1.144763	1.160564	1.173659	-3.5	-2.2	-1.1
0.6	1.303370	1.245248	1.268245	7.287556	-4.5	-2.7	-1.2
0.7	1.488234	1.483155	1.437816	1.467902	-0.3	-3.4	-1.4
0.8	1.815976	1.747479	1.733496	1.786292	-3.8	-4.5	-1.6
0.9	2.579413	2.271758	2.400426	2.522210	-11.9	-6.9	-2.2

Table 4. Comparison of the stress intensity factors $K(y)$ calculated in this sfudy at $y=0$ and $y=1/2$ ($y=x_2/a_0$) for an internal planar elliptic crack in a plate-under uniform tension σ_0 with the corresponding values $\bar{K}(y)$ given in Ref. 4; $K_0 = \sigma_0\sqrt{\pi L_0/2}$.

L_0/h	a_0/L_0	y	$K(y)/K_0$	$\bar{K}(y)/K_0$	$\frac{\bar{K}-K}{\bar{K}}$ 100
0.1	0.5	0	0.916	0.637	43.7
		1/2	0.868	0.637	36.2
	1.0	0	0.955	0.827	15.5
		1/2	0.896	0.785	14.2
	2.0	0	0.976	0.935	4.3
		1/2	0.911	0.875	4.1
	3.0	0	0.983	0.967	1.7
		1/2	0.916	0.902	1.6
	4.0	0	0.987	0.980	0.6
		1/2	0.919	0.914	0.5
	10.0	0	0.993	0.999	-0.6
		1/2	0.923	0.930	-0.7
0.2	0.5	0	0.862	0.638	35.1
		1/2	0.827	0.638	29.6
	1.0	0	0.931	0.830	12.2
		1/2	0.880	0.788	11.6
	2.0	0	0.971	0.942	3.1
					3.1
	3.0	0	0.986	0.976	1.0
		1/2	0.918	0.910	0.9

Table 4 - cont.

L_o/h	a_o/L_o	Y	$K(y)/K_o$	$\bar{K}(y)/K_o$	$\frac{\bar{K}-K}{\bar{K}}$ 100
0.2	4.0	0 1/2	0.993 0.923	0.991 0.923	0.2 0.0
	10.0	0 1/2	1.007 0.933	1.013 0.942	-0.6 -1.0
0.3	0.5	0 1/2	0.824 0.796	0.641 0.640	28.6 24.4
	1.0	0 1/2	0.920 0.871	0.837 0.794	9.9 9.8
	2.0	0 1/2	0.979 0.914	0.957 0.893	2.3 2.3
	3.0	0 1/2	1.001 0.930	0.996 0.927	0.5 0.3
	4.0	0 1/2	1.012 0.937	1.014 0.942	-0.2 -0.5
	10.0	0 1/2	1.034 0.952	1.041 0.966	-0.7 -1.5
0.4	0.5	0 1/2	0.798 0.775	0.645 0.644	23.6 20.3
	1.0	0 1/2	0.920 0.871	0.851 0.804	8.1 8.3
	2.0	0 1/2	1.000 0.929	0.984 0.915	1.6 1.6
	3.0	0 1/2	1.030 0.950	1.031 0.955	-0.1 -0.4

Table 4 - cont.

L_o/h	a_o/L_o	Y	$K(y)/K_o$	$\bar{K}(y)/K_o$	$\frac{\bar{K}-K}{K}$ 100
0.4	4.0	0 1/2	1.047 0.961	1.054 0.974	-0.7 -1.3
	10.0	0 1/2	1.078 0.982	1.091 1.005	-1.2 -2.3
0.5	0.5	0 1/2	0.783 0.761	0.654 0.650	19.8 17.2
	1.0	0 1/2	0.932 0.880	0.874 0.821	6.7 7.3
	2.0	0 1/2	1.036 0.956	1.030 0.949	0.6 0.7
	3.0	0 1/2	1.078 0.984	1.090 0.998	-1.1 -1.4
	4.0	0 1/2	1.101 0.998	1.121 1.023	-1.8 -2.4
	10.0	0 1/2	1.145 7.025	1.172 1.063	-2.4 -3.5
0.6	0.5	0 1/2	0.779 0.756	0.667 0.658	16.9 14.9
	1.0	0 1/2	0.960 0.901	0.911 0.846	5.4 6.4
	2.0	0 1/2	1,095 0.997	1.103 0.999	-0.8 -0.2
	3.0	0 1/2	1.151 1.033	1.183 1.061	-2.7 -2.6
	4.0	0 1/2	1.183 1.052	1.225 1.092	-3.5 -3.6
	10.0	0 1/2	7.245 1.088	1.298 1.143	-4.0 -4.7

Table 4 - cont.

L_o/h	a_o/L_o	Y	$K(y)/K_o$	$\bar{K}(y)/K_o$	$\frac{\bar{K}-K}{K}$ 100
0.7	0.5	0	0.788	0.687	74.7
		1/2	0.760	0.671	13.3
	1.0	0	1.009	0.968	4.3
		1/2	0.935	0.882	6.0
	2.0	0	7.187	1.273	-2.2
		1/2	1.058	1.067	-0.8
	3.0	0	1.266	1.322	-4.2
		1/2	1.106	1.144	-3.3
	4.0	0	1.310	1.381	-5.1
		1/2	1.132	1.783	-4.4
	10.0	0	1.403	1.483	-5.4
		1/2	1.179	1.242	-5.7
0.8	0.5	0	0.818	0.737	14.1
		1/2	0.777	0.686	72.9
	1.0	0	1.096	1.051	4.3
		3/2	0.991	0.930	6.6
	2.0	0	1.341	1.372	-2.3
		1/2	7.152	1.152	0.0
	3.0	0	7.457	1.521	-4.3
		1/2	1.218	1.245	-2.2
	4.0	0	1.525	1.603	-4.9
		1/2	1.253	1.290	-2.9
	10.0	0	1.674	7.747	-4.2
		1/2	1.318	1.349	-2.3

Table 4 - cont.

$-\theta/h$	a_o/L_o	y	$K(y)/K_o$	$\bar{K}(y)/K_o$	$\frac{\bar{K}-K}{\bar{K}}$ 100
1.9	0.5	0	0.905	0.759	19.3
		1/2	0.813	0.709	14.7
	1.0	0	1.284	1.167	10.0
		1/2	1.086	0.987	10.1
	2.0	0	1.661	1.594	4.2
		1/2	1.310	1.246	5.1
	3.0	0	1.858	7.799	3.3
		1/2	1.405	1.347	4.2
	4.0	0	1.981	1.912	3.6
		1/2	1.456	1.392	4.6

elliptic crack are consistently smaller than the plane strain values K_∞; $K(L_0)\to K_\infty$ as $a_0/L_0\to\infty$, and despite the approximate nature of the line spring method used to calculate $K(L_0)$ the relative error is surprisingly small.

Extensive results and formulas developed from the numerical solution obtained from a finite element method for an internal elliptic crack in a plate under tension are given in [4]. Figures 2-9 and Table 4 show the comparison of the stress intensity factors obtained from this study with those generated from the formulas given in [4]. Again K_∞ is the corresponding plane strain value given by Table 1 or Eq. (4) and the normalizing stress intensity factor is $K_0 = \sigma_0\sqrt{\pi L_0/2}$. The table gives the stress intensity factors calculated at $y = 0$ (the mid-section of the ellipse) and $y = 1/2$ (or $x_2 = a_0/2$). The table and the figures show that with the exception of relatively small values of a_0/L_0 at small L_0/h ratios (for which physically the line-spring is really not a suitable model) the agreement is generally good.

Another comparison with the previous finite element results [5] is shown in Table 5. It should be noted in the results given in Table 5

Table 5. Comparison of the stress intensity factors $K(L_0)$ calculated in this study at the midsection of an internal planar elliptic crack in a plate under uniform tension σ_0 with the corresponding results $\bar{K}$ given in [5]; $K_0=\sigma_0\sqrt{\pi L_0/2}$, $y=x_2/a_0=\cos\theta$ (Eqs. 6-8), $L_0/h=0.75$, $a_0/L_0=1.25$.

θ	y	$\bar{K}/K_0$	$K(L_0)/K_0$	$100\,\frac{K-\bar{K}}{\bar{K}}$
90°	0	0.985	1.120	13.7
80°	0.174	0.971	1.103	13.6
70°	0.342	0.944	1.052	11.4
60°	0.500	0.898	0.973	8.4
45°	0.707	0.810	0.832	2.7
40°	0.766	0.770	0.742	-3.6

L_o/h	Y	a_o/L_o					
		0.5	1.0	2.0	3.0	4.0	10.0
0.1	0	0.975	1.015	1.053	1.078	1.098	1.172
	0.6	0.946	1.001	1.046	1.073	1.095	1.170
0.2	0	0.931	0.991	1.033	1.055	1.071	1.134
	0.6	0.879	0.962	1.018	1.045	1.064	1.131
0.3	0	0.901	0.988	1.040	1.064	1.080	1.137
	0.6	0.831	0.943	1.017	1.048	1.069	1.133
0.4	0	0.883	0.998	1.067	1.096	1.113	1.169
	0.6	0.798	0.938	1.033	1.073	1.096	1.162
0.5	0	0.875	1.024	1.115	1.151	1.172	1.231
	0.6	0.777	0.947	1.068	1.118	1.147	1.221
3.6	0	0.879	1.068	1.192	1.239	1.266	1.333
	0.6	0.768	0.973	1.128	1.193	1.230	1.318
3.7	0	0.899	1.142	1.313	1.378	1.416	1.500
	0.6	0.774	1.023	1.225	7.313	1.364	1.478
1.8	0	0.946	1.269	1.520	1.623	1.680	1.800
	0.6	0.803	1.116	1.393	1.522	1.597	1.764
1.9	0	1.068	1.542	1.969	2.162	2.271	2.496
	0.6	0.892	1.326	1.760	1.981	2.115	2.420

Table 7. Normalized stress intensity factors $K(y)/K_0$ in a plate containing a symmetrically located elliptic or rectangular planar crack and subjected to pure bending M_0; $y=x_2/a_0$, $K_0 = (6M_0/h^2)\sqrt{\pi L_0/2}$.

		ELLIPTIC CRACK				RECTANGULAR CRACK			
L_0/h	y	a_0/L_0				a_0/L_0			
		0.5	1.0	2.0	4.0	0.5	1.0	2.0	4.0
0.1	0.0	0.296	0.297	0.297	0.297	0.353	0.369	0.382	0.390
	0.2	0.288	0.288	0.289	0.289	0.353	0.369	0.382	0.390
	0.4	0.261	0.261	0.261	0.262	0.353	0.369	0.382	0.390
	0.6	0.214	0.214	0.214	0.214	0.353	0.369	0.382	0.390
	0.8	0.135	0.135	0.135	0.135	0.352	0.369	0.382	0.390
	0.9	0.090	0.090	0.090	0.090	0.351	0.368	0.381	0.390
0.3	0.0	0.788	0.834	0.859	0.873	0.860	0.896	0.929	0.969
	0.2	0.775	0.816	0.838	0.850	0.858	0.895	0.928	0.969
	0.4	0.728	0.756	0.770	0.778	0.850	0.891	0.927	0.968
	0.6	0.635	0.643	0.646	0.649	0.832	0.882	0.923	0.966
	0.8	0.432	0.427	0.419	0.417	0.773	0.849	0.907	0.958
	0.9	0.290	0.280	0.275	0.273	0.685	0.790	0.873	0.942
0.5	0.0	0.948	1.122	1.248	1.341	1.107	1.264	1.373	1.467
	0.2	0.948	1.113	1.231	1.317	1.098	7.258	1.370	1.464
	0.4	0.941	1.079	1.171	1.234	1.064	1.236	1.357	1.454
	0.6	0.912	0.994	1.040	1.069	0.993	1.186	1.327	1.433
	0.8	0.746	0.736	0.723	0.715	0.827	1.044	1.232	1.374
	0.9	0.556	0.511	0.485	0.472	0.657	0.871	1.087	1.275
0.7	0.0	0.846	1.119	1.382	1.643	1.001	1.313	1.613	1.904
	0.2	0.856	1.125	1.381	1.629	0.987	1.301	1.602	1.893
	0.4	0.884	1.139	1.369	1.574	0.944	7.261	1.567	1.857
	0.6	0.934	1.147	1.318	1.446	0.856	1.174	1.491	1.782
	0.8	0.929	1.010	1.046	1.056	0.675	0.971	1.300	1.611
	0.9	0.836	0.802	0.761	0.728	0.514	0.765	1.074	1.400
0.9	0.0	0.712	1.031	1.436	1.952	0.825	1.224	1.758	2.457
	0.2	0.713	1.029	1.422	1.915	0.813	1.210	1.739	2.431
	0.4	0.739	1.051	1.421	1.852	0.772	1.162	1.679	2.345
	0.6	0.814	1.118	1.447	1.772	0.692	1.065	1.559	2.180
	0.8	0.926	7.149	1.329	1.443	0.534	0.854	1.300	1.853
	0.9	0.979	1.067	1.086	1.070	0.400	0.656	1.036	1.632

a_0/L_0 = 7.25 is relatively small for the line spring model to be effective. Despite that the relative error does not seem to be very high. The angle e shown in the table is the parameter defining the point on the ellipse (see (7)).

Table 6 shows the stress intensity factors in a plate containing a rectangular planar crack and subjected to uniform tension σ_0. Referring to Fig. lb, in this case the crack is defined by

$$-\frac{L_0}{2} < x_3 < \frac{L_0}{2} \quad , \quad -a_0 < x_2 < a_0$$

One may note that, as expected, the stress intensity factors for the rectangular crack are generally somewhat greater than the corresponding values for an elliptic crack.

The results for a plate containing a symmetrically located (Fig. lb) elliptic or rectangular planar crack and subjected to pure bending (Fig. la) are given in Table 7. It should again be noted that for larger values of y and smaller values of a_0/L_0 the line-spring model which is used to calculate these results is not a suitable model. Table 7 shows the stress intensity factor along the border of the crack on the tension side of the plate. On the compression side the stress intensity factors have the same values with a negative sign. Under pure bending since the crack faces on the compression side of the plate would close, the results given in the table cannot be used separately. The results are, of course, useful and valid if the plate is subjected to tension, as well as bending in such a way that the superimposed stress intensity factor is positive everywhere.

4. References

1. F. Delale and F. Erdogan, "Line Spring Model for Surface Cracks in a Reissner Plate", Int. J. Engng. Science, Vol. 19, pp. 1331-1340, 1981.

2. F. Delale and F. Erdogan, "Application of the Line Spring Model to a Cylindrical Shell Containing a Circumferential or an Axial Part-Through Crack", J. Appl. Mech., Vol. 49, Trans. ASME, pp. 97-102, 1982.

3. A.C. Kaya and F. Erdogan, "Stress Intensity Factors and COD in an Orthotropic Strip", Int. J. of Fracture, Vol. 16, pp. 171-190, 1980.

4. J.C. Newman, Jr. and I.S. Raju, "Stress Intensity Factor Equations for Cracks in Three-Dimensional Finite Bodies", ASTM STP-791, pp. 238-265, 1983.

5. T. Nishioka and S.N. Atluri, "Analytical Solution for Embedded Elliptical Cracks, and Finite Element Alternating Method for Elliptical Surface Cracks, Subjected to Arbitrary Loadings", Engineering Fracture Mechanics, Vol. 17, pp. 247-268, 1983.

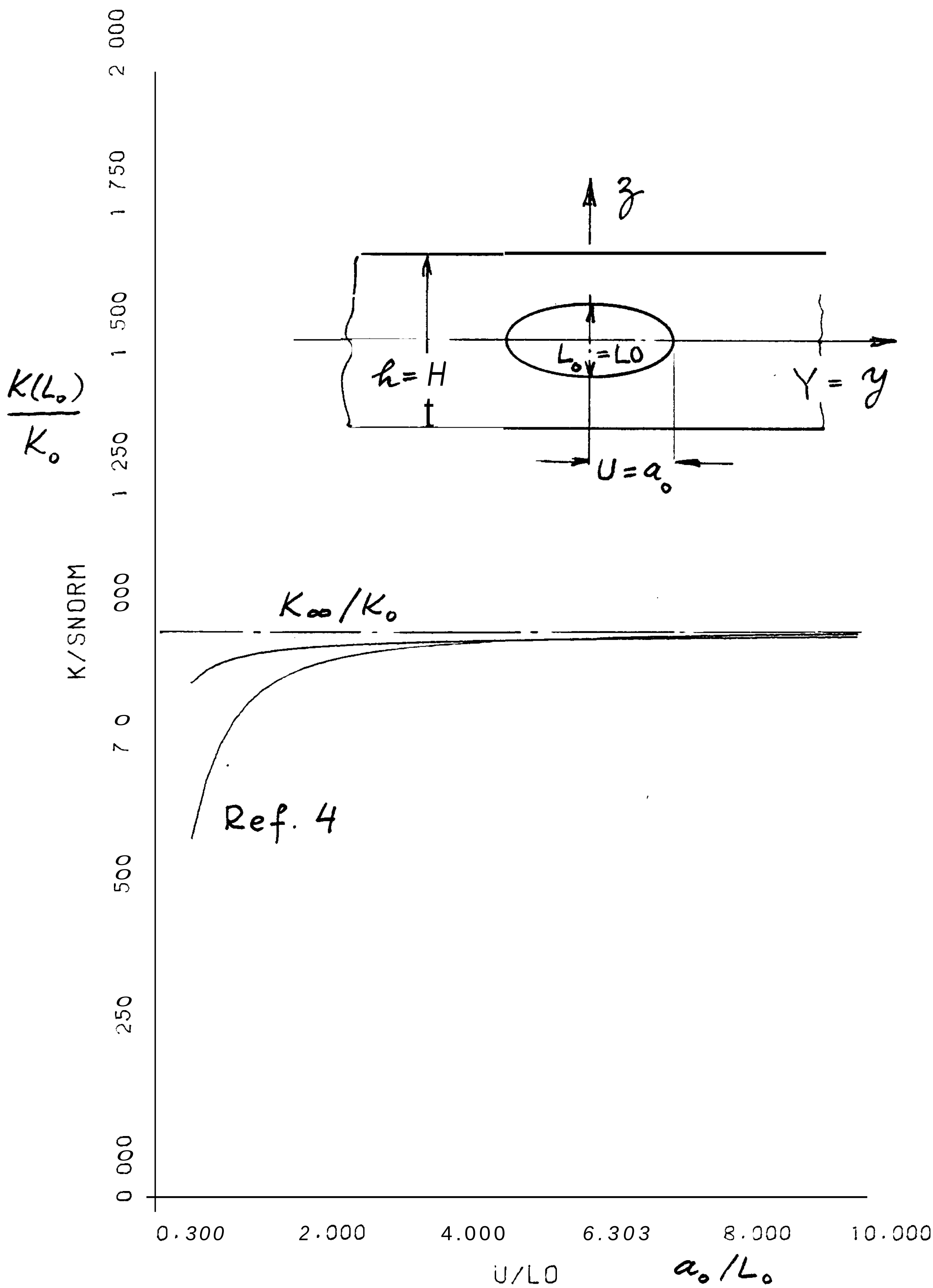

Fig. 2 Stress intensity factor at the midsection of a planar elliptic crack in a plate subjected to uniform tension $\sigma_{xx}^{\infty} = \sigma_0$ for $L_0/h = 0.1$; $K_0 = \sigma_0\sqrt{\pi L_0/2}$, K_∞ the plane strain value (for which $a_0 = \infty$).

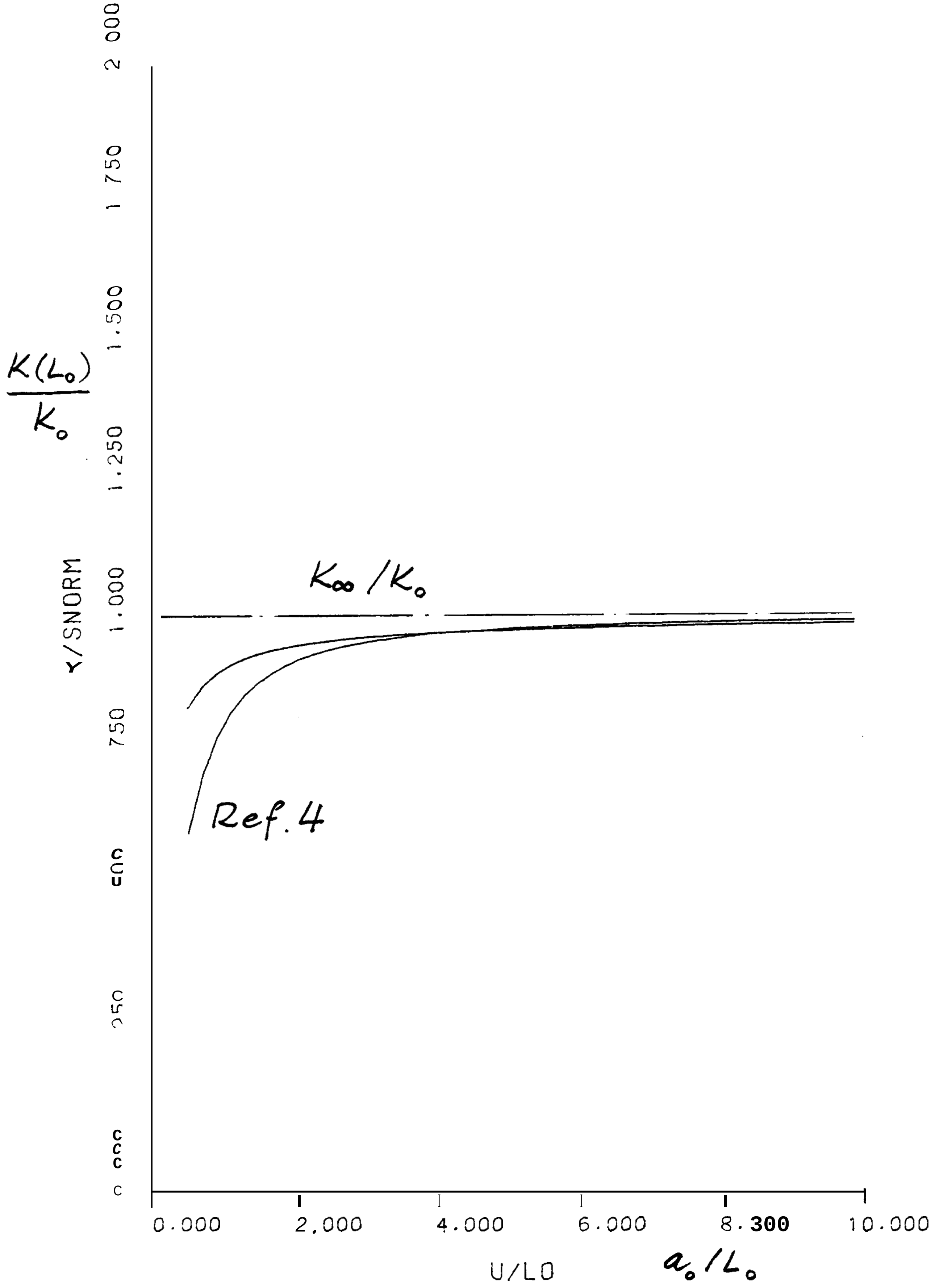

Fig. 3 Stress intensity factor at the midsection of a planar elliptic crack in a plate subjected to uniform tension $\sigma_{xx}^{\infty} = \sigma_0$ for $L_0/h = 0.2$; $K_0 = \sigma_0\sqrt{\pi L_0/2}$, K_∞ the plane strain value (for which $a_0 = \infty$).

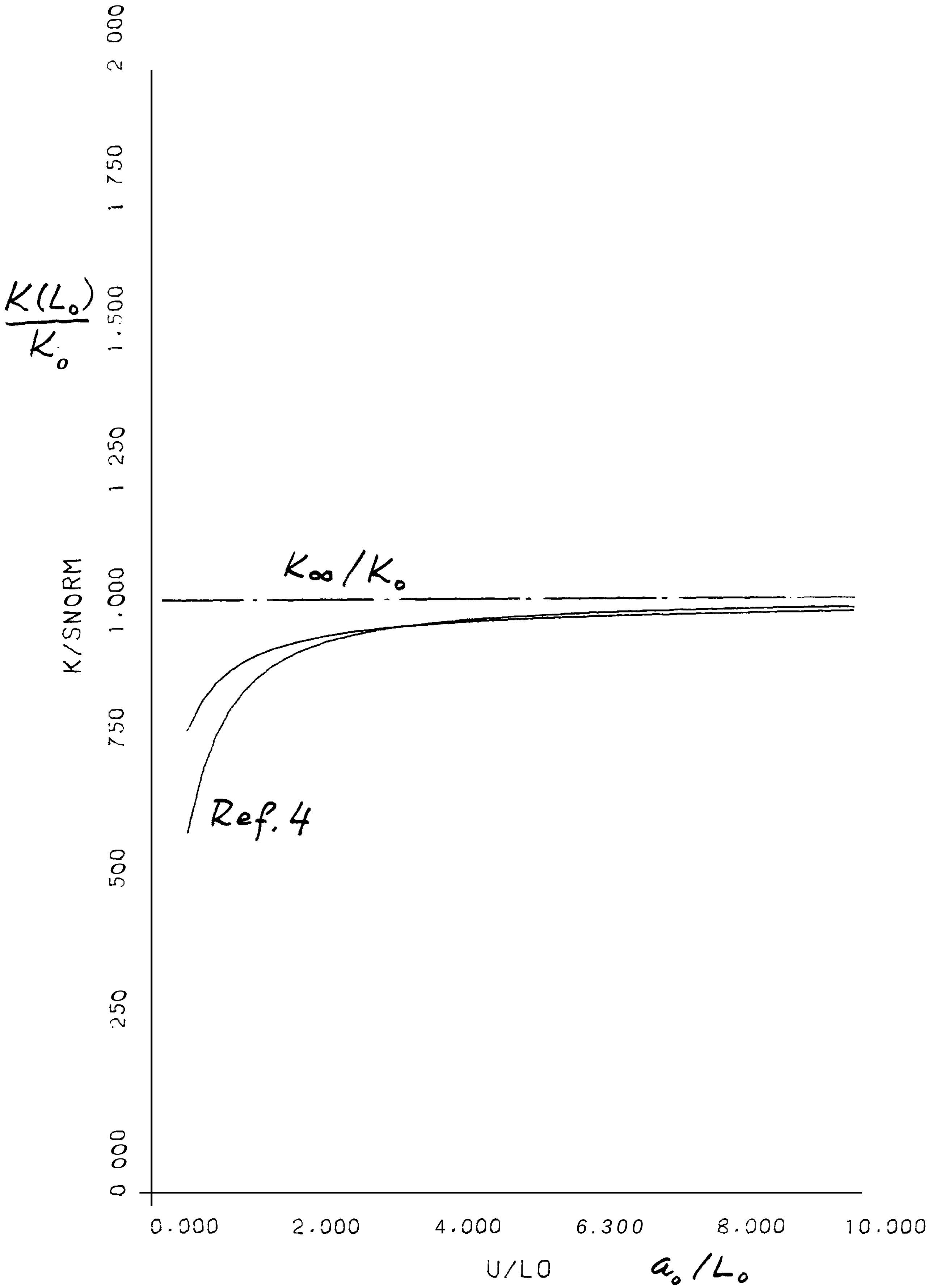

Fig. 4 Stress intensity factor at the midsection of a planar elliptic crack in a plate subjected to uniform tension $\sigma_{xx}^{\infty} = \sigma_0$ for $L_0/h = 0.3$; $K_0 = \sigma_0\sqrt{\pi L_0/2}$, K_∞ the plane strain value (for which $a_0 = \infty$).

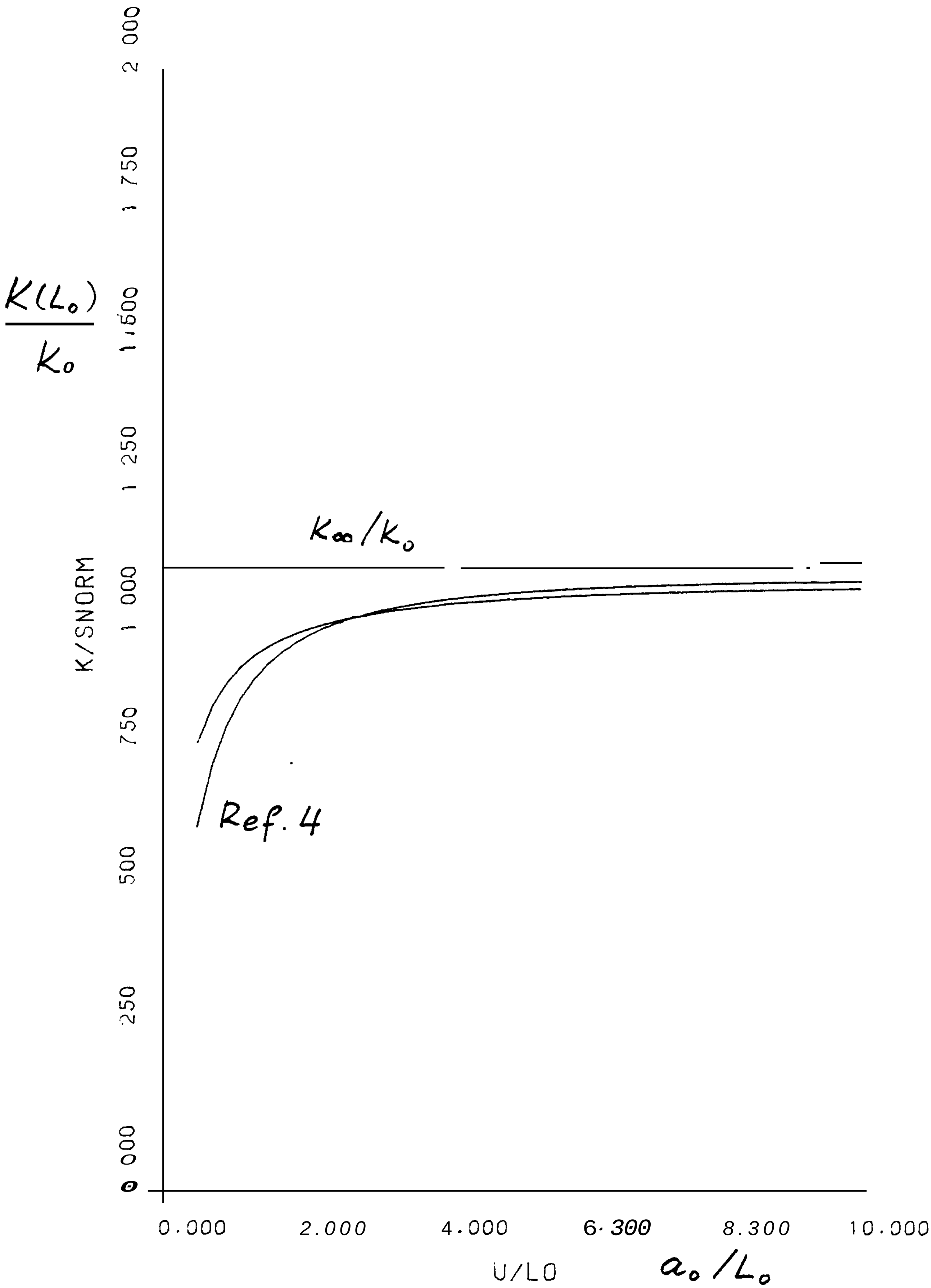

Fig. 5 Stress intensity factor at the midsection of a planar elliptic crack in a plate subjected to uniform tension $\sigma_{xx}^{\infty} = \sigma_0$ for $L_0/h = 0.4$; $K_0 = \sigma_0\sqrt{\pi L_0/2}$, K_∞ the plane strain value (for which $a_0 = \infty$).

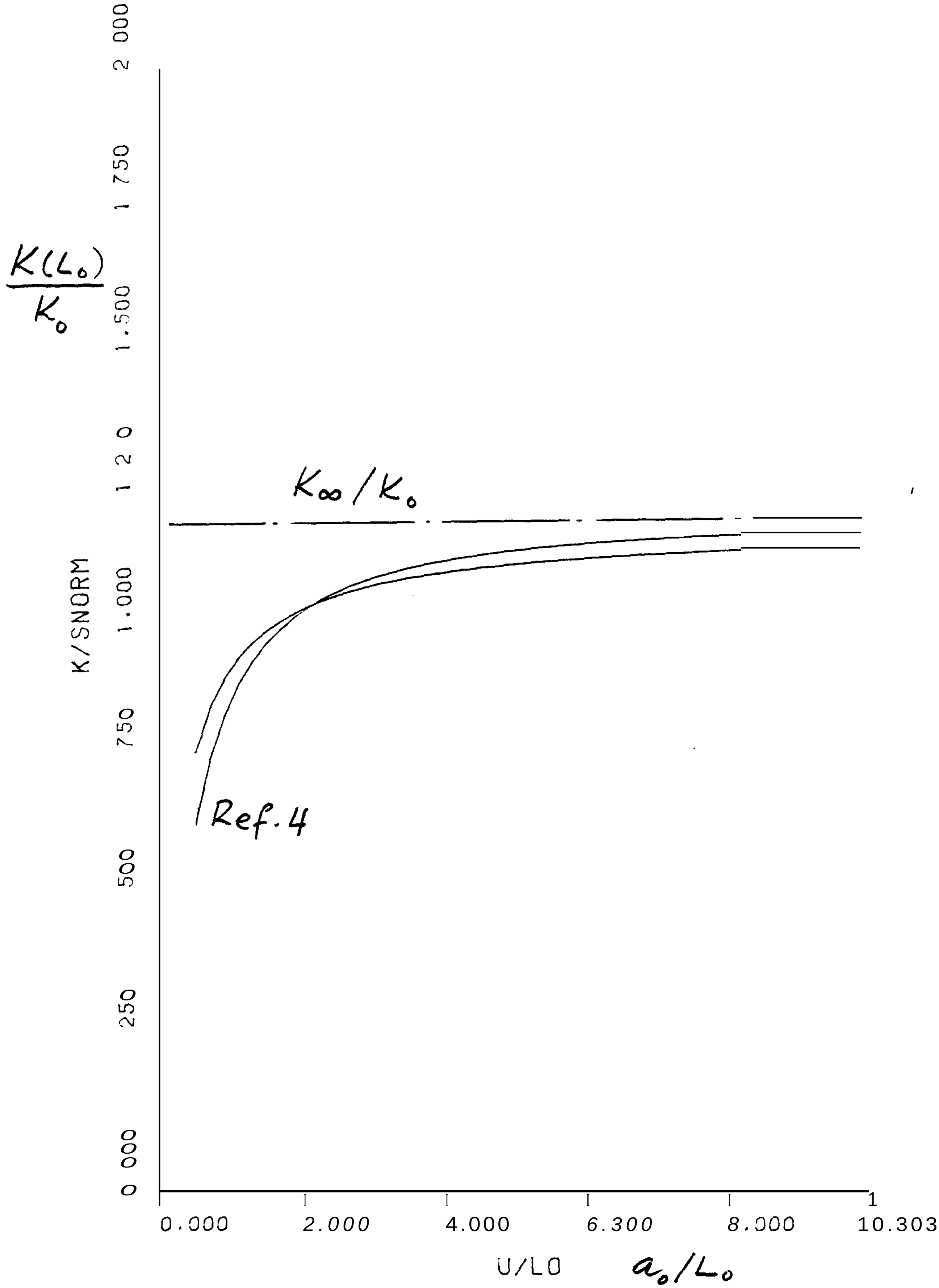

Fig. 6 Stress intensity factor at the midsection of a planar elliptic crack in a plate subjected to uniform tension $\sigma_{xx}^{\infty} = \sigma_0$ for $L_0/h = 0.5$; $K_0 = \sigma_0\sqrt{\pi L_0/2}$, K_∞ the plane strain value (for which $a_0 = \infty$).

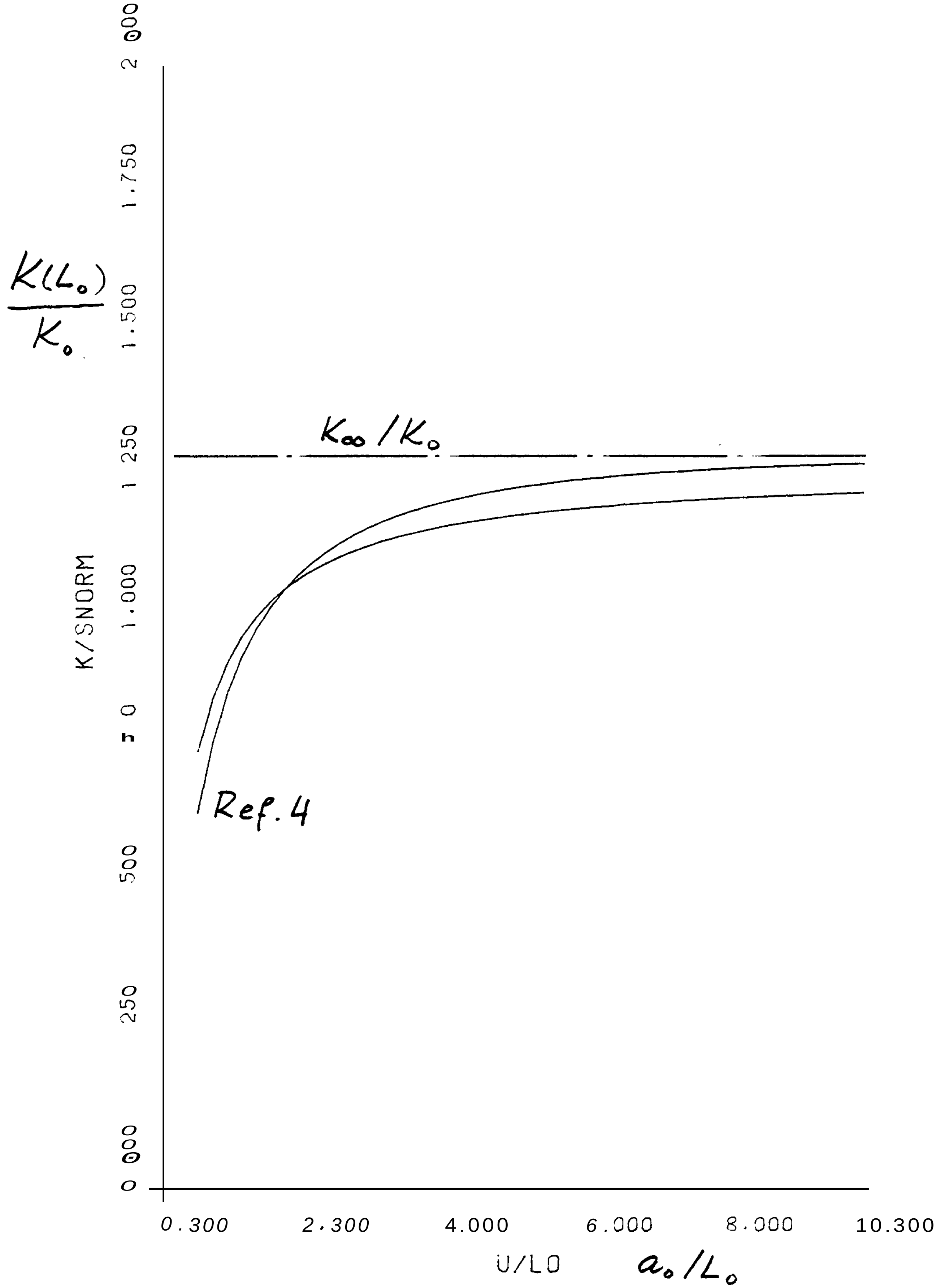

Fig. 7 Stress intensity factor at the midsection of a planar elliptic crack in a plate subjected to uniform tension $\sigma_{xx}^{\infty} = \sigma_0$ for $L_0/h = 0.6$; $K_0 = \sigma_0\sqrt{\pi L_0/2}$, K_∞ the plane strain value (for which $a_0 = \infty$).

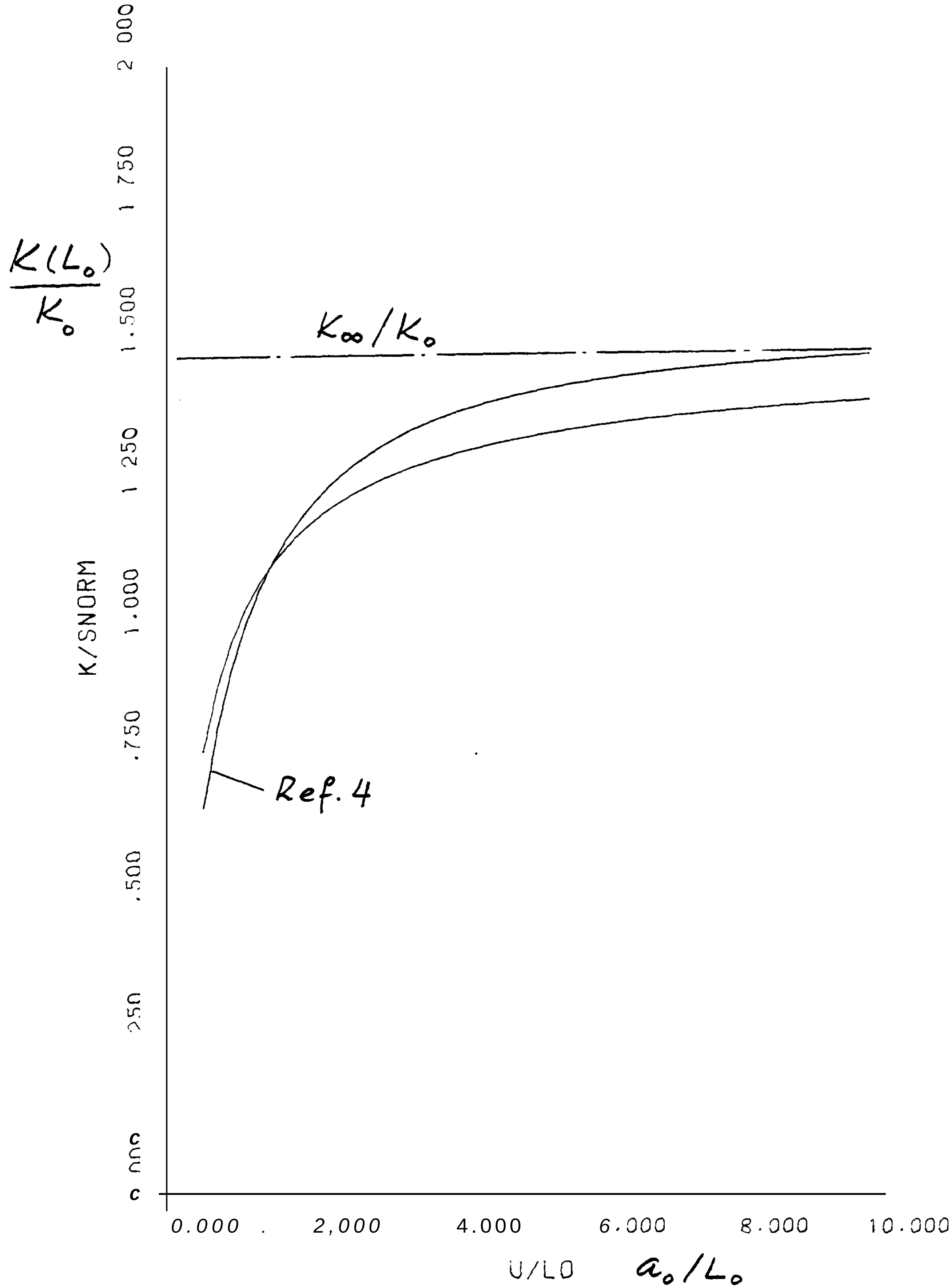

Fig. 8 Stress intensity factor at the midsection of a planar elliptic crack in a plate subjected to uniform tension $\sigma_{xx}^{\infty} = \sigma_0$ for $L_0/h = 0.7$; $K_0 = \sigma_0\sqrt{\pi L_0/2}$, K_∞ the plane strain value (for which $a_0 = \infty$).

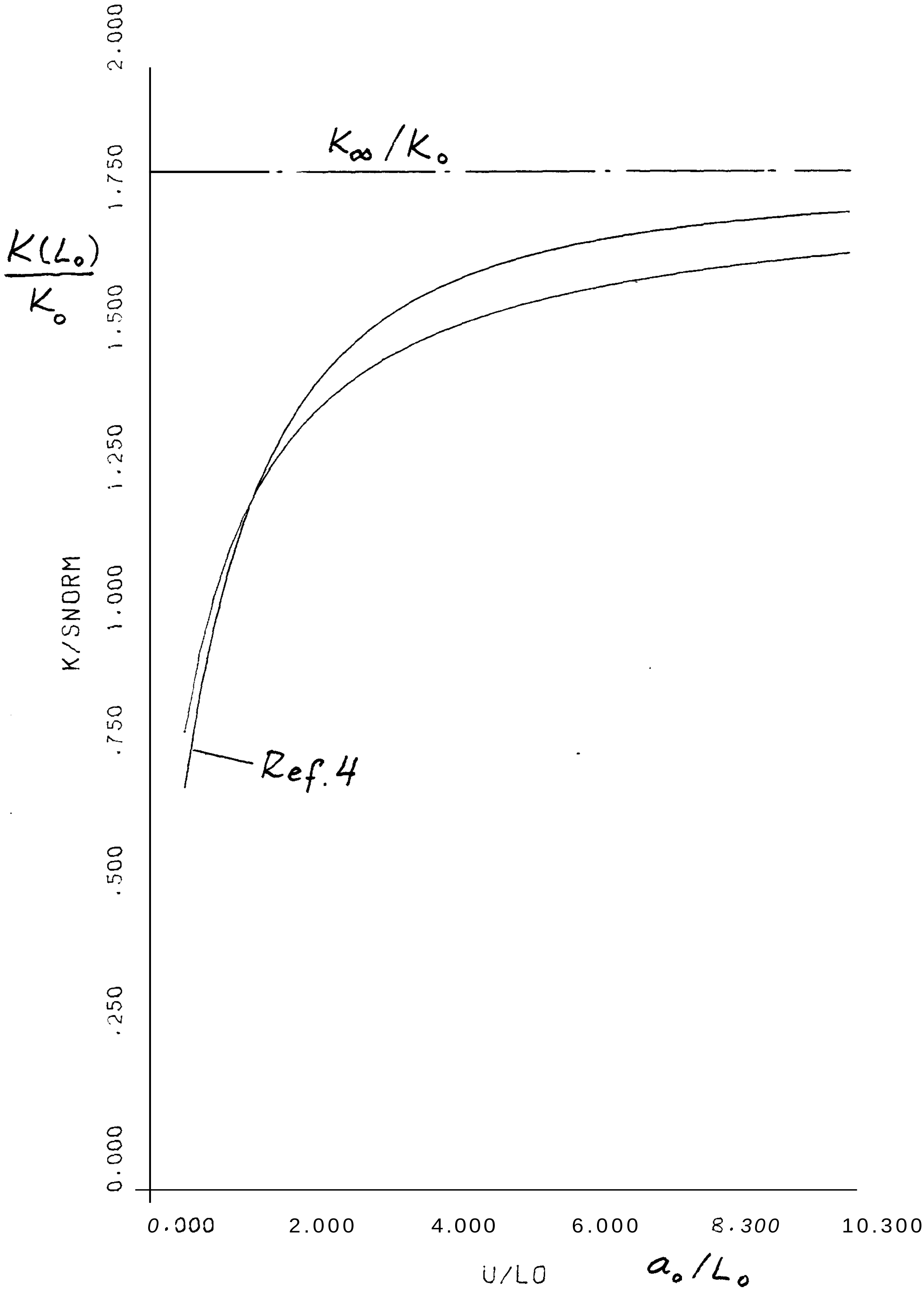

Fig. 9 Stress intensity factor at the midsection of a planar elliptic crack in a plate subjected to uniform tension $\sigma_{xx}^{\infty} = \sigma_0$ for $L_0/h = 0.8$; $K_0 = \sigma_0\sqrt{\pi L_0/2}$, K the plane strain value (for which $a_0 = \infty$).